


**Teleportation of a quantum particle in a potential via quantum Zeno dynamics**Miguel A. Porras *Grupo de Sistemas Complejos, ETSIME, Universidad Politécnica de Madrid, Rios Rosas 21, 28003 Madrid, Spain*

Miguel Casado-Álvarez

*Departamento de Energía y Combustibles, ETSIME, Universidad Politécnica de Madrid, Rios Rosas 21, 28003 Madrid, Spain*Isabel Gonzalo *Departamento de Óptica, Facultad de Ciencias Físicas, Universidad Complutense de Madrid, Ciudad Universitaria s/n, 28040 Madrid, Spain*

(Received 14 May 2023; accepted 20 February 2024; published 12 March 2024)

We report on the possibility of teleportation of a quantum particle, a distinctly different phenomenon from the teleportation of a quantum state through entanglement. With the first meaning, teleportation is theoretically possible by placing the particle initially at rest (with a certain uncertainty) out of any equilibrium point of a potential well or barrier and by frequently monitoring whether the particle remains at rest. This quantum Zeno dynamics inhibits acceleration, and features disappearance from the classical turning point and appearance in another turning point, if there is any other, with a probability that approaches unity by increasing the frequency of the measurements. This phenomenon has all the ingredients attributed in science fiction to teleportation: The particle is always at rest, cannot be found in the path between the two turning points, and saves travel time. We discuss the feasibility, in principle, of teleportation of electrons, protons, and other particles, and conclude its increasing impracticability as the particle gets heavier. Nevertheless, our paper establishes a basis for further studies in which the projective and instantaneous measurements are replaced by more realistic models.

DOI: [10.1103/PhysRevA.109.032207](https://doi.org/10.1103/PhysRevA.109.032207)**I. INTRODUCTION**

It has been known since the 1990s that quantum teleportation is a technique of transmitting quantum information from an emitter to a receiver over a distance. It requires quantum entanglement, and therefore several particles [1–3]. The possibility of teleportation with the meaning prior to the above achievements, i.e., the teleportation of a single object, has deserved very little attention. Without a scientific basis, the hypothetical teleportation of a particle relies on science fiction literature since the 19th century, on popular culture, and since the advent of cinema on science fiction movies. It would involve (1) disappearance of the particle from one location of space, (2) appearance in another distant location, (3) being permanently at rest, and (4) following no path joining the two locations. Teleportation is, also hypothetically, a way to save time on the trip. To our knowledge, only Ref. [4] discusses the possibility of teleportation in a fractional Schrödinger equation, approached by the high-speed limit of relativistic quantum mechanics, and relates teleportation with superconductivity and superfluidity. Also in Ref. [4], and more closely related to this paper, the possibility of teleportation in the standard, nonrelativistic Schrödinger equation with measurements of wave-function parity is briefly discussed.

Here we report on the possibility of teleportation of a quantum particle with all the above science fiction characteristics. Teleportation is shown here to result from a peculiar quantum Zeno dynamics (QZD). Quantum Zeno dynamics [5–9] must be distinguished from its predecessor, the quantum Zeno

effect [10–13]. In the quantum Zeno effect, the temporal evolution of a quantum system is interleaved by measurements of whether the state remains the initial one, which results in freezing the evolution in the initial state as the measurements are more frequent. In QZD, measurements ascertain whether the state remains in a set of states, or a multidimensional subspace of the system Hilbert space. The QZD has been studied theoretically [5–9], and has been recently realized in a rubidium Bose-Einstein condensate in a five-level Hilbert space [14].

Beyond a discrete and finite number of states, most of the studies of QZD in an infinite-dimensional Hilbert space involve repeated measurements of position which, being necessarily imprecise, monitor whether the particle remains in the region of space, say  $\Delta x$ , where it is initially found. Reference [15] demonstrates that von Neumann projective measurements of position lead to a unitary evolution confined in the subspace defined by  $\Delta x$  with Dirichlet boundary conditions in the limit of continuous measurements, i.e., when the number of measurements  $N$  approaches infinity. Different QZD with position measurements have been studied [16–18] and featured different effects such as inhibition of wave-packet spreading of a particle at rest [19] and stopping a freely moving particle (the Zeno arrow) in a Schrödinger cat state [20].

More recently, Porras *et al.* [21] have analyzed the conjugate QZD involving repeated measurements of momentum. Specifically, frequently monitoring whether the momentum of a particle directed towards a potential barrier remains positive results in freezing the momentum direction and hence, in a

Zeno-assisted quantum tunneling, with tunneling probability approaching unity as the number of measurements increases.

The QZD leading to teleportation is that of a particle initially at rest, that is,  $\langle v \rangle = 0$  with a certain uncertainty  $\Delta v$ , out of an equilibrium point in a potential, hence experiencing a force at a classical turning point, whose state of rest within the uncertainty  $\Delta v$  is frequently monitored. The resulting QZD tends to keep the particle at rest, i.e., the quantum state in the subspace of velocities  $|v| < \Delta v$ , with higher probability with growing number of measurements, and despite the force acting on the particle.

We find that the way of remaining at rest is at least a bit striking (see video in Supplemental Material [22]). The particle disappears from its initial location while appearing on another classical turning point, if there is any other, exhibiting all the above-mentioned characteristics of teleportation. When the number of measurements  $N$  increases, the probability of teleportation approaches unity in a teleportation time that is independent of  $N$ . The teleportation time is proportional to the mass and  $\Delta v$ , but shorter as the force is stronger, and can be made much shorter than the time taken by the particle to travel up to the other turning point (see also video in Supplemental Material [22]).

We demonstrate the extremely small probability flux in the path between the two turning points, which amounts to a violation of the equation of continuity for the probability in this QZD, and rigorously supports referring to it as teleportation. Eventually, we examine how the mass affects the teleportation probability with different schemes of measurements. The conclusion here is that teleportation remains possible, in principle, for heavier particles, but becomes increasingly difficult and completely impracticable for macroscopic objects.

## II. ZENO DYNAMICS OF A PARTICLE IN A POTENTIAL MONITORED AT REST

We start with the Schrödinger equation for a particle of mass  $m$  in a potential  $V$ ,  $i\hbar\partial|\psi\rangle/\partial t = \hat{H}|\psi\rangle = (\hat{p}^2/2m)|\psi\rangle + \hat{V}|\psi\rangle$  written for the wave function  $\psi(x, t) = \langle x|\psi\rangle$  in one dimension and in atomic units ( $\hbar = 1, m_e = 1$ ) as

$$i\frac{\partial\psi}{\partial t} = -\frac{1}{2m}\frac{\partial^2\psi}{\partial x^2} + V(x)\psi. \quad (1)$$

For simplicity we will take symmetric potentials about  $x = 0$ . The particle is initially at rest and localized about a position  $x_0 = \langle x \rangle$  different from an equilibrium point, i.e., at a classical turning point experiencing a force, and such that there is only one other turning point  $-x_0$ . For the moment we consider a potential well. Later we show that the same results hold almost identically for the well inverted to a barrier, and also almost identically for a harmonic potential and for the inverted harmonic potential. Being initially at rest means  $\langle v \rangle = 0$  with a certain uncertainty  $\Delta v$ . Considering initial Gaussian-like wave functions  $\psi(x, 0) = \langle x|\psi_0\rangle$  and  $\psi(p, 0) = \langle p|\psi_0\rangle$  of half Gaussian widths ( $1/e^2$  decay in probability)  $\Delta x$  and  $\Delta p$ , such minimal wave packets verify  $\Delta x\Delta p = 2$ ; hence, given  $\Delta v$ ,  $\Delta x = 2/m\Delta v$ , but this is only a choice to fix ideas.

We next consider the following QZD. In a given time interval  $T$ , the particle wave function is left to evolve in small time intervals  $\Delta t = T/N$  according to Eq. (1), interleaved

with measurements of whether the particle remains at rest with the same uncertainty  $\Delta v$  about zero as initially. The number of measurements of velocity is then  $N$ . They are modeled as projections of the state onto the subspace of velocities  $|v| < \Delta v$ , or equivalently onto the subspace of momenta  $|p| < m\Delta v$ . We consider only positive outcomes ( $|v| < \Delta v$ ) in all the measurements, i.e., the measurements are selective, and wonder about the probability  $P_N^{(S)}$  that all measurements are positive. Upon a negative outcome the measurements are terminated.

The QZD with these selective measurements can then be symbolized as

$$|\phi_N\rangle = \frac{1}{\sqrt{P_N}}\Pi e^{-i\hat{H}\Delta t} \dots \frac{1}{\sqrt{P_2}}\Pi e^{-i\hat{H}\Delta t} \frac{1}{\sqrt{P_1}}\Pi e^{-i\hat{H}\Delta t} |\psi_0\rangle, \quad (2)$$

where  $\Pi = \int_{-m\Delta v}^{m\Delta v} |p\rangle\langle p| dp$  is the projector onto  $[-m\Delta v, m\Delta v]$ , and  $P_n$  is the probability that the velocity is in  $[-\Delta v, \Delta v]$  (momentum in  $[-m\Delta v, m\Delta v]$ ) at the  $n$  intermediate measurement, so that the factors  $1/\sqrt{P_n}$  normalize the state after each projective measurement. After the  $N$  measurement at time  $T$ , the probability that all outcomes were positive is the product  $P_N^{(S)} = P_1 P_2 \dots P_N$ . To obtain  $P_N^{(S)}$ , however, it is traditional in QZD, and faster computationally, to evaluate the un-normalized state

$$|\psi_N\rangle = \Pi e^{-i\hat{H}\Delta t} \overset{N-3 \text{ times}}{\dots\dots\dots} \Pi e^{-i\hat{H}\Delta t} \Pi e^{-i\hat{H}\Delta t} |\psi_0\rangle, \quad (3)$$

which is obviously related to the normalized state  $|\phi_N\rangle$  in (2) by  $|\psi_N\rangle = \sqrt{P_1 P_2 \dots P_N} |\phi_N\rangle$ , and whose norm,

$$\langle \psi_N | \psi_N \rangle = P_1 P_2 \dots P_N = P_N^{(S)}, \quad (4)$$

yields directly the probability  $P_N^{(S)}$  that all outcomes were positive. In all figures, the un-normalized state at any intermediate step  $n$  is represented since its norm informs us about the probability that the velocity remains in  $\Delta v$  about  $\langle v \rangle = 0$  at the intermediate step  $n$ .

We have implemented the above QZD in a numerical code, where unitary evolutions in  $\Delta t$  are performed using a standard symmetrized split step Fourier method to solve the Schrödinger equation, and measurements by truncating the wave function in momentum representation outside  $[-m\Delta v, m\Delta v]$ . In the symmetrized split step Fourier method, the time interval  $\Delta t$  is divided in small steps  $h$ . The effect of the kinetic-energy term in (1) in half a step  $h/2$  is trivially evaluated in Fourier space through a fast Fourier transform, the effect of the potential term in (1) in the interval  $h$  is applied at the midpoint  $h/2$  in direct space after inverse fast Fourier transform, and the effect of the kinetic energy in the remainder  $h/2$  is again evaluated as above in Fourier space [23].

For the Gaussian potential well  $V(x) = -V_0 \exp(-x^2/x_p^2)$  of width  $x_p$ , the initial location is far from the equilibrium point  $x = 0$  by setting  $x_0 \sim x_p$ . This choice also implies a significant force, which accelerates the phenomenon of interest, as seen below. Also, the uncertainty  $\Delta v$  is chosen such that  $\Delta x = 2/\Delta p = 2/m\Delta v$  is much smaller than  $x_p$  so that the probability of being located at the other turning point is zero for all practical purposes.

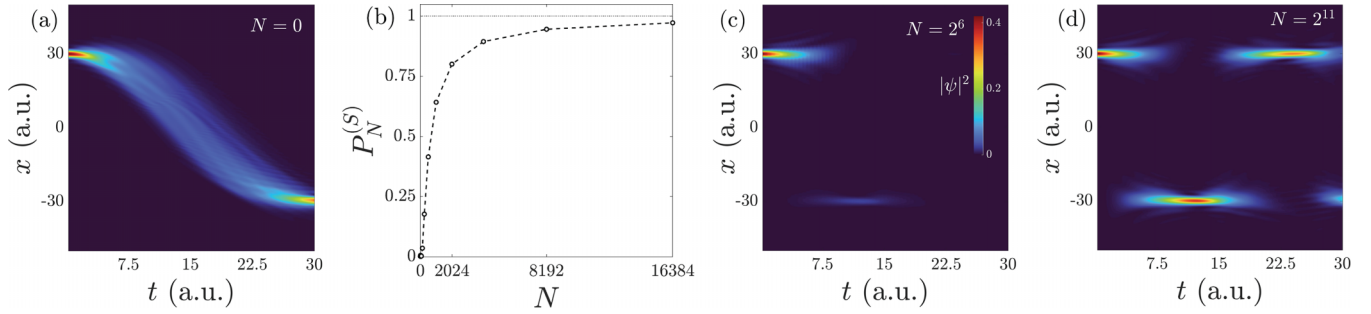


FIG. 1. [(a), (c), (d)] Contour plots of the probability density as a function of time for a particle of mass  $m = 1$  initially at the state  $\psi(x, 0) = (1/\pi)^{1/4} \exp[-(x - x_0)^2/2]$ ,  $x_0 = 30$  in the potential well  $V(x) = -V_0 \exp(-x^2/x_p^2)$ ,  $x_p = 30$  and  $V_0 = 10$ . All quantities are in atomic units. (a) Without any measurement. (b) Probability that the particle remains at rest with uncertainty  $\Delta v = \sqrt{2}$  at the final time  $T = 30$  as a function of number of measurements  $N$ . [(c), (d)] The same as (a) but with the indicated number of measurements.

Typical results for  $m = 1$  (an electron) are shown in Fig. 1. Without measurements, the wave function oscillates in the well, as seen in Fig. 1(a) [the Gaussian well is represented in Fig. 2(a)]. With measurements of whether the particle remains at rest within  $\Delta v$ , the particle tends to remain at rest with probability  $P_N^{(s)}$  approaching unity as the number of measurements  $N$  within the time  $T$  increases, as seen in Fig. 1(b). This QZD then features freezing the velocity about zero against the permanent force acting on it. Figures 1(c) and 1(d) show the striking way in which the particle stays still: The particle “finds” the other turning point where it can stay still,  $-x_0$ ,

and appears and disappears periodically in  $-x_0$  and  $x_0$  with a period substantially independent of  $N$  and ostensibly smaller than the natural period of the oscillations.

In Fig. 2(a) different potential wells and barriers are depicted. Figure 2(b) shows that this phenomenon is almost identical for a Gaussian well and the inverted Gaussian well to form a Gaussian barrier. Also, Figs. 2(c) and 2(d) illustrate the existence of the same phenomenon in a harmonic potential and inverted harmonic potential. In all three cases the initial wave function corresponds to the same particle at rest as in Fig. 1 and the particle experiences a force of the same magnitude (the absolute values of the slopes at  $x_0$  are the same).

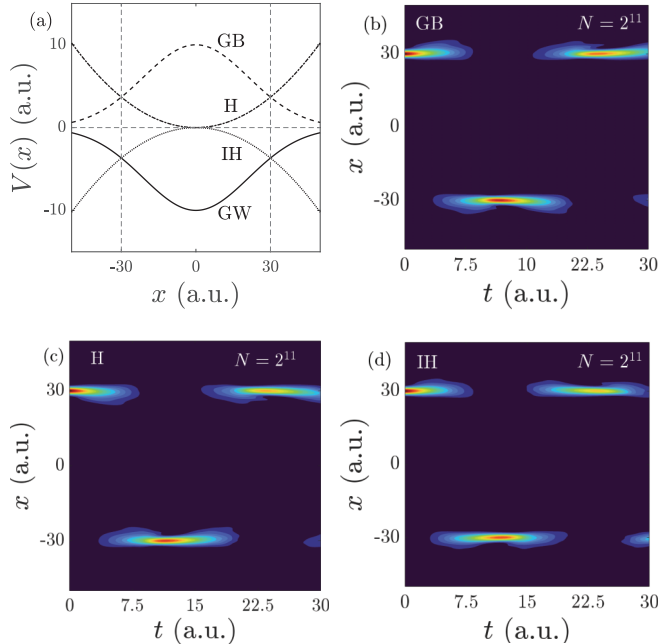


FIG. 2. (a) Gaussian well  $V(x) = -V_0 \exp(-x^2/x_p^2)$  (GW), Gaussian barrier  $V(x) = V_0 \exp(-x^2/x_p^2)$  (GB), harmonic potential  $V(x) = ax^2$  (H), and inverted harmonic potential  $V(x) = -ax^2$  (IH). In all them  $V_0 = 10$ ,  $x_p = 30$ , and we chose  $a = eV_0/(x_p^2)$  so that the magnitude of the force at the initial position  $x_0 = x_p$  is the same. [(b)–(d)] Contour plots of the probability density as functions of time for the same particle and initial state as in Fig. 1 with  $N = 2^{11}$  measurements of whether the particle remains at rest with uncertainty  $\Delta v = \sqrt{2}$  within the total time  $T = 30$ .

### III. TELEPORTATION

From now on we set  $T$  equal to the time that the particle takes to teleport from one to another turning point, or teleportation time  $T_{\text{telep}}$ , defined as the time at which the probability density at  $-x_0$  is maximum. Since no appreciable norm is left at  $T_{\text{telep}}$  at  $x_0$ , the probability  $P_N^{(s)}$  is the probability of teleportation. A closer look at examples allows us to identify the mechanism of teleportation and to estimate  $T_{\text{telep}}$ .

#### A. Teleportation mechanism

Figure 3 shows the probability densities in position and momentum spaces at the selected times (a)  $t = 0$ , (b)  $T_{\text{telep}}/2$ , and (c)  $T_{\text{telep}}$  for the same initial state and potential well as in Fig. 1. The number of measurements  $N = 2^{10}$  is high, hence the probability of teleportation  $P_N^{(s)} = 0.93$  is also high. A video of the whole dynamics can be found in the Supplemental Material [22]. At no time does  $|\psi(x, t)|^2$  take significant values in the path between  $x_0$  and  $-x_0$  (first row in Fig. 3). We discard a significant probability current or flux  $j(x, t) = (1/m)\text{Im}\{\psi^* \partial \psi / \partial x\}$  between  $x_0$  and  $-x_0$  (second row). This point is further discussed below.

The mechanism of teleportation can be understood from the dynamics of the wave function in momentum representation. We observe in the third row of Fig. 3 that the repeated measurements create a sharp potential well in momentum space extending from  $-\Delta p = -m\Delta v$  to  $\Delta p = m\Delta v$ . In the limit of continuous measurements,  $N \rightarrow \infty$ , the well would become infinitely high, with the momentum wave function  $\hat{\psi}(p)$  satisfying Dirichlet boundary conditions at

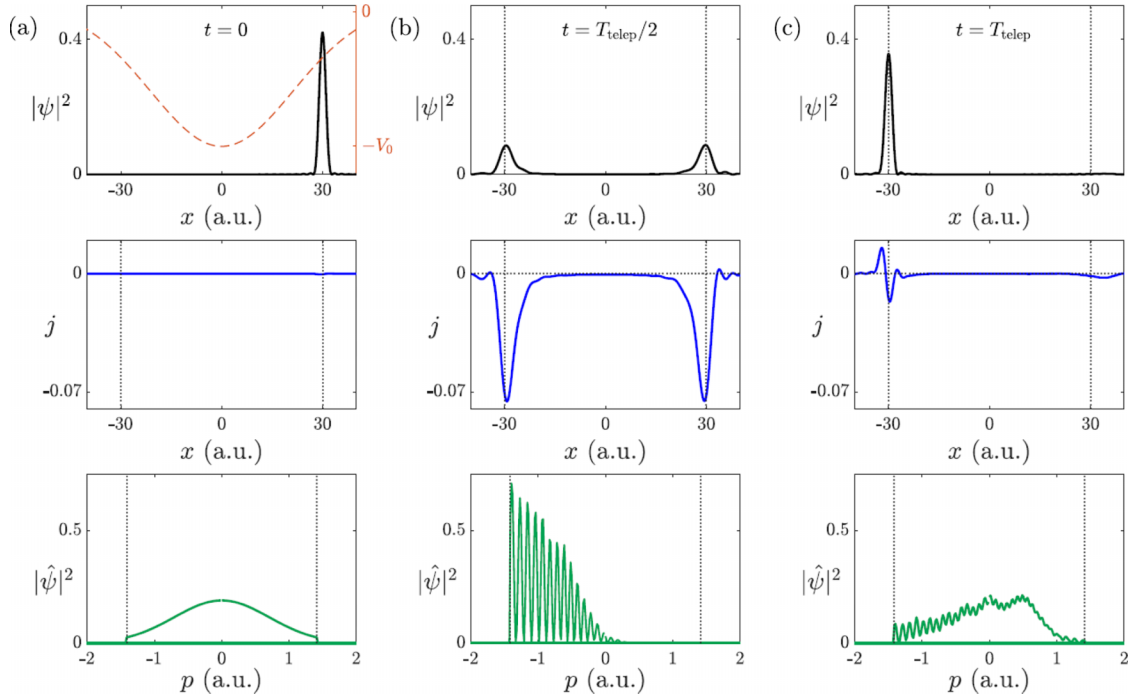


FIG. 3. For the same Gaussian potential well and initial wave function as in Fig. 1, probability density (first row), probability current (second row), and momentum probability density (third row), at (a)  $t = 0$ , (b)  $t = T_{\text{telep}}/2$ , and (c)  $t = T_{\text{telep}} = 11.533$  a.u. The number of measurements is  $N = 2^{10}$  and the final probability of finding the particle at  $-x_0$  is  $P_N^{(s)} = 0.93$ . The Gaussian potential well is depicted as a dashed curve in panel (a), top.

$-\Delta p = -m\Delta v$  and  $\Delta p = m\Delta v$ , in a similar way as in Ref. [15] for position measurements. With finite measurements the reflections produce norm losses that are smaller as  $N$  increases. We also observe that the reflection is about the time  $T_{\text{telep}}/2$  at which the particle is located at  $x_0$  and  $-x_0$  with approximately equal probabilities, and that the return to the original location of the momentum wave function about  $p = 0$  coincides with  $T_{\text{telep}}$  at which the particle is only located at  $-x_0$ .

Thus, writing the initial wave function as  $\psi(x, 0) = \psi(x - x_0)$ , or  $\hat{\psi}(p, 0) = \hat{\psi}(p)e^{-ix_0p}$  in momentum representation, the wave function transforms upon reflection into a superposition  $\alpha\hat{\psi}(p)e^{-ix_0p} + \beta\hat{\psi}(p)e^{ix_0p}$  of left and right moving momentum wave functions, which originates the observed interference fringes, with decreasing  $\alpha$  and increasing  $\beta$  as the reflection takes place, or equivalently, a position wave function  $\alpha\psi(x - x_0) + \beta\psi(x + x_0)$  disappearing from  $x_0$  and appearing in  $-x_0$ .

The expectation value of momentum in this reflection follows approximately the laws of classical mechanics. Since the particle does not appreciably move from  $x_0$  while it disappears, the force acting on it takes the approximately constant value  $F = -V'(x_0)$ , where  $V' = dV/dx$ . With constant force, the mean momentum as a function of time is then  $\langle p \rangle \simeq -V'(x_0)t$ , which equated to  $-\Delta p$  yields the reflection time as  $\Delta p/V'(x_0)$ . Similarly, from the reflection onwards, the mean momentum changes with time as  $\langle p \rangle \simeq -\Delta p - V'(-x_0)t = -\Delta p + V'(x_0)t$  for a symmetric potential, which equated to zero when the momentum wave function comes back to the center yields again a time  $\Delta p/V'(x_0)$ . The teleportation time is then twice this quantity. The same reasonings apply to the

potential barrier obtained from inversion of the well, except that reflection occurs on the right of the sharp potential well in momentum space with the positive force  $F = -V'(x_0) > 0$ . Thus, for well or barrier, the teleportation time is

$$T_{\text{telep}} \simeq \frac{2\Delta p}{|V'(x_0)|} = \frac{2m\Delta v}{|V'(x_0)|}. \quad (5)$$

This expression provides an excellent approximation to the time at which the probability of finding the particle at its original location is zero. Small deviations are due to the slight deviation of the force from  $-V'(x_0)$  when the particle slightly moves at  $x_0$  or at  $-x_0$ . For a nonsymmetric potential the teleportation time would be  $m\Delta v/|V'(x_0)| + m\Delta v/|V'(x_1)|$ , where  $x_1$  is the second turning point. It is also clear from (5) that a force is essential to teleportation. In particular, if the particle is placed at an equilibrium point, teleportation to another equilibrium point requires infinite time, i.e., does not occur at all.

Figure 4 illustrates that the teleportation mechanism continues to work, although with less efficiency, when unsharp projections are performed. With the unsharp projective measurements in Fig. 4(a), Eq. (5) continues to yield the correct teleportation time, but the probability is about one half that with sharp measurements, as seen in Fig. 4(b).

## B. Teleportation as a violation of the continuity equation

The idea of teleportation, or translation at rest along no path, can more rigorously be associated with the extinction of the probability of presence in a region of space and emergence of probability in another separate region without



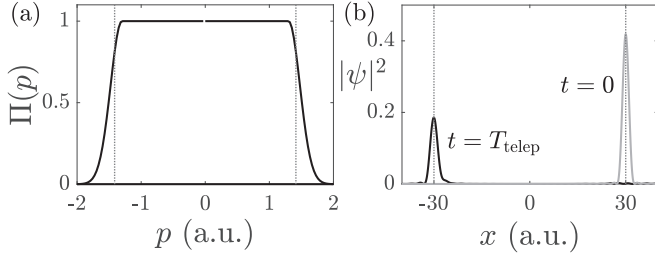


FIG. 4. Teleportation with unsharp measurements of whether the particle remains at rest with uncertainty  $\Delta v = \sqrt{2}$ . (a) Unsharp projector  $\Pi(p) = 1$  if  $|p| \leq 1.3$ ,  $\exp[-(p - 1.3)^2/0.25^2]$  if  $p > 1.3$ , and  $\exp[-(p + 1.3)^2/0.25^2]$  if  $p < -1.3$ . (b) For the same Gaussian well and initial wave function as in Figs. 2 and 3, probability density at the teleportation time  $t = T_{\text{telep}} = 11.533$  a.u. with  $N = 2^{10}$  unsharp measurements. The teleportation probability has decreased from 0.93 to 0.57.

probability flux through their boundaries. This is a violation of the continuity equation. While the continuity equation is always satisfied in Schrödinger evolution alone, it is not necessarily satisfied in a QZD.

In one dimension the continuity equation reads  $\partial|\psi|^2/\partial t + \partial j/\partial x = 0$ , or in integral form,  $(d/dt) \int_a^b |\psi|^2 dx = j(a, t) - j(b, t)$ , stating that the variation of the probability in the interval  $[a, b]$  per unit time must be due to a probability flux across its boundaries. We take here the relevant interval as  $[0, \infty)$  since the particle is initially at the positive  $x$  axis. Therefore

$$\frac{d}{dt} \int_0^\infty |\psi(x, t)|^2 dx = j(0, t) - j(0, \infty) = j(0, t). \quad (6)$$

Further integration in time and some rearrangement lead to

$$1 - \int_0^\infty |\psi(x, t)|^2 dx = - \int_0^t j(0, t) dt, \quad (7)$$

expressing that, in Schrödinger evolution, the decrement of the probability in  $[0, \infty)$  [left-hand side of (7)] is due to the outgoing probability through  $x = 0$  (right-hand side). Without measurements, this is illustrated in Fig. 5(a) with the same example as in Fig. 1(a) (half an oscillation in the potential well). The norm is constant in time (black solid curve), the decrement of the probability of finding the particle in  $[0, \infty)$  is complete (dashed curve), and it coincides with the outgoing probability through  $x = 0$  (gray solid curve). Figure 5(b) shows the same quantities but for the example of Fig. 3 with  $N = 2^{11}$  measurements. In the QZD the norm is almost constant (would be exactly constant in the limit  $N \rightarrow \infty$ ), and the decrement of probability of finding the particle in  $[0, \infty)$  is also complete, but this decrement is not equal to the outgoing probability through  $x = 0$  (gray horizontal curve), which is negligible at any time. Hence (6) and (7) are not satisfied, supporting that the particle does not follow a path, but disappears from  $[0, \infty)$ , and, the norm being almost unity at the end, the particle is located in  $(-\infty, 0]$ .

The outgoing probability from  $[0, \infty)$  through  $x = 0$  (gray horizontal curve) is negligible compared to the probability appearing in  $(-\infty, 0]$ , but is not exactly zero. A closer examination of the probability density (e.g., in log scale) shows a myriad of ripples filling the whole well at very low level,

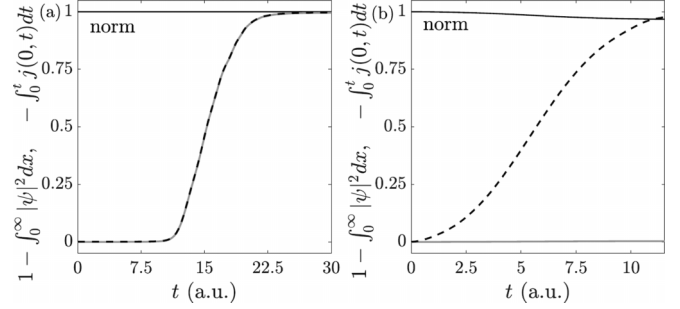


FIG. 5. (a) For the example of Fig. 1(a) (no measurements) in the same potential well, the norm is unity (black solid curve), and the decrement of the probability of finding the particle in  $[0, \infty)$  (dashed curve) is equal to the outgoing probability through  $x = 0$  (gray solid curve), as required by the continuity equation. (b) For the same example in Fig. 3 with  $N = 2^{11}$  measurements, the decrement of the probability of finding the particle in  $[0, \infty)$  (dashed curve) is not equal to the outgoing probability through  $x = 0$  (gray solid curve).

of the order of  $10^{-5}$  in Fig. 3. These are caused by the measurement operator  $\Pi$ , which in momentum representation is the truncation  $\Pi(p)\hat{\psi}(p) = \hat{\psi}(p)$  if  $|p| \leq [-m\Delta v, m\Delta v]$ , 0 otherwise, and in position representation the convolution  $\Pi(x)\psi(x) = 2(m\Delta v/\hbar) \sin(m\Delta vx/\hbar)/(m\Delta vx/\hbar) * \psi(x)$ . In Fig. 5(a) the outgoing probability from  $[0, \infty)$  through  $x = 0$  due to these ripples during  $T_{\text{telep}}$  is  $-\int_0^{T_{\text{telep}}} j(0, t) dt = 0.0029$ , which is indeed very small compared to  $P_N^{(s)} = 0.9691$ . It can be said that actual teleportation probability is  $P_N^{(s)} + \int_0^{T_{\text{telep}}} j(0, t) dt$ , or 0.9662 in this example.

It is not surprising that the continuity equation is not satisfied in a QZD involving von Neumann measurements, where the role of the measurement apparatus is to project the wave function in a subspace of momenta: The continuity equation derives from the Schrödinger equation for the temporal evolution without any type of measurement. What is surprising is the way it is violated: The outgoing probability through  $x = 0$  might just have differed from the decrement of probability, but in this QZD the outgoing probability is negligible, supporting the idea of teleportation.

#### IV. TELEPORTATION OF HEAVIER PARTICLES AND THE CLASSICAL LIMIT

The above results simply show the theoretical possibility of teleportation according to standard quantum mechanics. Hereinafter we discuss whether this effect could be possible, also in principle, in hypothetical experiments monitoring rest with typical uncertainties of velocity of particles at rest of different masses, and ultimately, with macroscopic particles.

For an electron  $\Delta v = \sqrt{2}$  a.u. ( $\approx 10^6$  m/s) and  $\Delta x = \sqrt{2}$  a.u. ( $\approx 10^{-10}$  m) in the above examples may be reasonable, but not for heavier particles that tend to slow down and to localize. This is reflected by the Boltzmann distribution of velocities  $\propto e^{-mv^2/a}$  of one-dimensional particles ( $a$  would be  $a = 2k_B\mathcal{T}$ , where  $k_B$  is the Boltzmann constant and  $\mathcal{T}$  is the temperature), of mean value  $\langle v \rangle = 0$  and width  $v_{\text{th}} = \sqrt{a/m}$ . If these are statistically expected values of classical particles at

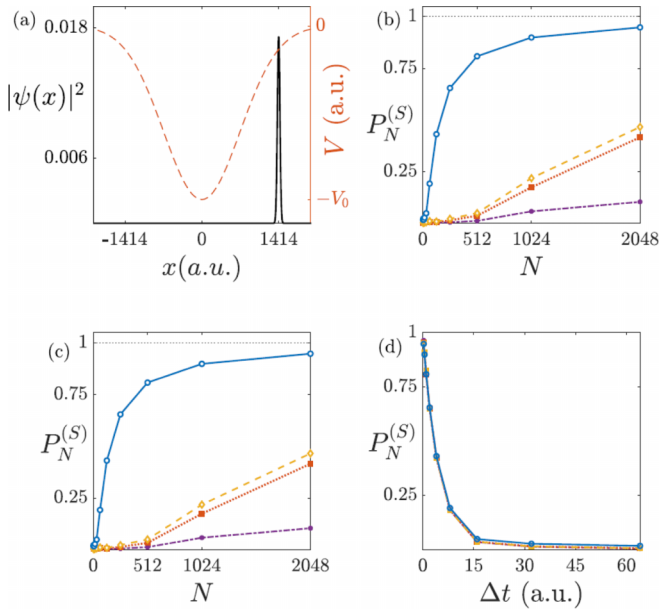


FIG. 6. Probability of teleportation in different measurements schemes for four particles: electron ( $m = 1$ , open circles), muon ( $m = 206.767$ , diamonds), pion ( $m = 273.767$ , squares), and proton ( $m = 1836$ , closed circles). (a) Initial wave function for the electron  $\psi(x, 0) = (2/\pi\Delta x^2)^{1/4} \exp[-[(x - x_0)/\Delta x]^2]$ , with  $x_0 = 1414.2$  and  $\Delta x = 2/\sqrt{am}$ ,  $a = 1.856 \times 10^{-3}$  a.u. (the initial wave functions of the other three particles are narrower), and the potential well  $V(x) = -V_0 \exp(-x^2/x_p^2)$ ,  $x_p = 1000$ . All quantities are expressed in atomic units. (b) The potential depth is set to  $V_0 = 0.4396\sqrt{m/m_e}$ , where  $m_e = 1$  is the electron mass, so that it grows for heavier particles and all of them have the same teleportation time  $T_{\text{telep}} = 512$  a.u. (c) The potential depth  $V_0 = 0.4396$  is kept constant and therefore the teleportation time increases with mass as in Eq. (8),  $T_{\text{telep}} = 512, 7362, 8463,$  and  $21\,940$  a.u. (d) Teleportation times are the same as in panel (c), but the interval between measurements,  $\Delta t$ , is the same for all particles.

temperature  $\mathcal{T}$ , it is then reasonable to take for our initial pure state  $\Delta v = v_{\text{th}}$ , leading to  $\Delta p = \sqrt{am}$  and the increasingly localized wave function with  $\Delta x = 2/\sqrt{am}$ . Note however that this state does not represent a thermal particle, but simply that the statistical uncertainty is assigned to the quantum uncertainty. This assignment yields, e.g.,  $\Delta v \approx 9 \times 10^4$  m/s and  $\Delta x \approx 2 \times 10^{-9}$  m for an electron, and  $\Delta v \approx 9.2 \times 10^2$  m/s and  $\Delta x \approx 2 \times 6^{-11}$  m for a proton at room temperature.

The teleportation time (5) becomes

$$T_{\text{telep}} = \frac{\sqrt{4am}}{|V'(x_0)|}. \quad (8)$$

A particle with the above wave-function properties is placed in a potential well, as in Fig. 6(a). For a comparison of the behavior of particles of different masses, the potential has the same shape for all particles, and all particles are placed at the same position  $x_0$  for the teleportation distance  $2x_0$  to be the same.

We consider four particles of increasing mass. To strictly adhere to the QZD scheme, the teleportation time  $T_{\text{telep}}$  is the same for the four particles by making the potential depth  $V_0$  grow with mass. The location  $x_0$  is also chosen so that

$T_{\text{telep}} = 512$  a.u. is sufficiently long, making not completely unreasonable a high number of measurements; In the example of Fig. 6(b),  $N = 2^9$  measurements would correspond to a measurement each  $\Delta t = 1$  a.u., about 24 as. This figure shows the probability of teleportation as the number of measurements grows for an electron, a muon, a pion, and a proton. One could of course prolong the curves to a higher number of measurements and all curves will approach unity, but these curves suffice to illustrate the increasing difficulty of teleporting heavier particles.

We may also keep the same well depth for all four particles. Then the teleportation time increases with the square root of mass,  $T_{\text{telep}} = 512, 7362, 8463,$  and  $21\,940$  a.u. With the same conditions as in Figs. 6(a) and 6(b) except the constant depth  $V_0$ , Fig. 6(c) shows the probability of teleportation at each teleportation time for the same four particles. Again, heavier particles are teleported with less probability with each given number of measurements.

We may still argue that in the scheme in Fig. 6(c), with longer and longer teleportation times and the same number of measurements, the time interval  $\Delta t$  between them is longer. We then consider, as a third possibility, the probability of teleportation when  $\Delta t$  is kept constant for all four particles along the respective teleportation times. Figure 6(d) shows again the probability of teleportation for constant  $\Delta t$  during the respective teleportation times. In this case, all four particles teleport with almost equal probability approaching unity as  $\Delta t \rightarrow 0$ , and the same would happen for atoms and molecules, with the “only” added difficulty of sustaining the measurements for longer and longer times.

Ultimately, the coherent state of being located at  $x_0$  and at about  $-x_0$  at the same time will collapse to  $x_0$  or  $-x_0$  if any interaction with the environment (in addition to interactions involved in the velocity measurements in the QZD) would inform where the particle is located. With increasing environmental interactions of heavier particles and increasing teleportation times, the state will most likely collapse at the very beginning of the teleportation process to the state located at  $x_0$ .

Finally, it is of interest to consider the “velocity” of teleportation (although the particle is always at rest). A reasonable definition would be the distance between the original and final positions over the teleportation time,  $v_{\text{telep}} = 2x_0/T_{\text{telep}}$  in the above examples. This yields  $v_{\text{telep}} = 5.5$  a.u. for all particles in the scheme in Fig. 6(b), and  $v_{\text{telep}} = 5.5, 0.38, 0.33,$  and  $0.13$  a.u. for the four particles in the schemes in Figs. 6(b) and 6(c). These velocities are significantly smaller than the velocity of light  $c \simeq 137$  a.u., which justifies the use of the nonrelativistic Schrödinger equation. However, it is not difficult to conceive of situations in which  $v_{\text{telep}}$  is arbitrarily high. For example, setting  $V_0 = 10.9\sqrt{m/m_e}$  a.u. in the scheme in Fig. 6(b) yields  $v_{\text{telep}} = c$ , and arbitrarily superluminal teleportation velocities for higher  $V_0$ . These are unphysical situations in the frame of the Schrödinger equation that call for an analysis of teleportation from relativistic equations such as the Dirac equation.

## V. CONCLUSIONS

We have unveiled a mechanism in which a quantum particle at rest at a classical turning point of a potential, and

therefore subjected to a force, remains at rest more likely the more frequently it is measured if the particle remains at rest. This is an example of QZD which, interestingly, leads to the following phenomenon: teleportation of the quantum particle, whereby the particle appears and disappears from the location where it is at rest and appears at another location where it can be at rest, if there is any location. Disappearing and appearing means here that there is no appreciable probability flux exiting the boundaries of the original location or entering the boundaries of the final location. This entails a violation of the continuity equation of the probability density, which is, in our opinion, the fact that makes this phenomenon deserve the name “teleportation.” We have set realistic values of the involved physical quantities showing the increasing difficulty of performing teleportation as the particle gets heavier.

Nonselective measurements in this QZD, as in Refs. [21,24], have not been considered because the “no path” property is lost. While the probability of finding the particle at the other turning point would be higher than with selective measurements [21,24], the wave functions corresponding to negative outcomes tend to fill the path between the two turning points. Thus, QZD-assisted teleportation requires selective measurements.

We believe that the possibility of teleportation established here deserves further study with more realistic models of measurements and relativistic quantum equations. In particular, the impact of the Heisenberg position-momentum and

energy-time uncertainty relations on the feasibility of fast measurements should be analyzed. A possible implementation of teleportation could be based on the Doppler shift of scattered photons, whose frequencies would be differently shifted depending on whether the particle is at rest or not. Measurements should be insensitive to the position of the particle at the original location or at its teleportation destination, which would require photon wave packets longer than the potential dimensions,  $\approx 2x_p$  in our examples, which in turn appears to limit the repetition rate of the measurements to  $\Delta t \approx 2x_p/c$ . Increasing the repetition rate with shorter pulses would require erasing the position information carried by the photons (e.g., different travel times) with adequate experimental strategies. Finally, we insist that the teleportation of the mass of a particle described here must be clearly distinguished from the current studies and experiments of teleportation in quantum information.

### ACKNOWLEDGMENTS

The authors acknowledge helpful discussions with Alfredo Luis. M.A.P. acknowledges support from the Spanish Ministry of Science and Innovation, Gobierno de España, under Contract No. PID2021-122711NB-C21. M.C.-A. acknowledges support from grant “Beca de colaboración de formación” of the Universidad Politécnica de Madrid.

- 
- [1] C. H. Bennett, G. Brassard, C. Crépeau, R. Jozsa, A. Peres, and W. K. Wootters, Teleporting an unknown quantum state via dual classical and Einstein-Podolsky-Rosen channels, *Phys. Rev. Lett.* **70**, 1895 (1993).
  - [2] D. Bouwmeester, J.-W. Pan, K. Mattle, M. Eibl, H. Weinfurter, and A. Zeilinger, Experimental quantum teleportation, *Nature (London)* **390**, 575 (1997).
  - [3] S. Pirandola, J. Eisert, C. Weedbrook, A. Furusawa, and S. L. Braunstein, Advances in quantum teleportation, *Nat. Photon.* **9**, 641 (2015).
  - [4] Y. Wei, Comment on “Fractional quantum mechanics” and “Fractional Schrödinger equation,” *Phys. Rev. E* **93**, 066103 (2016).
  - [5] P. Facchi, V. Gorini, G. Marmo, S. Pascazio, and E. C. G. Sudarshan, Quantum Zeno dynamics, *Phys. Lett. A* **275**, 12 (2000).
  - [6] P. Facchi and S. Pascazio, Quantum Zeno dynamics: mathematical and physical aspects, *J. Phys. A* **41**, 493001 (2008).
  - [7] P. Facchi and S. Pascazio, Quantum Zeno subspaces, *Phys. Rev. Lett.* **89**, 080401 (2002).
  - [8] J. M. Raimond, P. Facchi, B. Peaudecerf, S. Pascazio, C. Sayrin, I. Dotsenko, S. Gleyzes, M. Brune, and S. Haroche, Quantum Zeno dynamics of a field in a cavity, *Phys. Rev. A* **86**, 032120 (2012).
  - [9] B. Militello, M. Scala, and A. Messina, Quantum Zeno subspaces induced by temperature, *Phys. Rev. A* **84**, 022106 (2011).
  - [10] B. Misra and E. C. G. Sudarshan, The Zeno’s paradox in quantum theory, *J. Math. Phys.* **18**, 756 (1977).
  - [11] W. M. Itano, D. J. Heinzen, J. J. Bollinger, and D. J. Wineland, Quantum Zeno effect, *Phys. Rev. A* **41**, 2295 (1990).
  - [12] M. C. Fischer, B. Gutiérrez-Medina, and M. G. Raizen, Observation of the quantum Zeno and anti-Zeno effects in an unstable system, *Phys. Rev. Lett.* **87**, 040402 (2001).
  - [13] S. Maniscalco, F. Francica, R. L. Zaffino, N. Lo Gullo, and F. Plastina, Protecting entanglement via the quantum Zeno effect, *Phys. Rev. Lett.* **100**, 090503 (2008).
  - [14] F. Schäfer, I. Herrera, S. Cherukattil, C. Lovecchio, F. S. Cataliotti, F. Caruso, and A. Smerzi, Experimental realization of quantum Zeno dynamics, *Nat. Commun.* **5**, 3194 (2014).
  - [15] P. Facchi, S. Pascazio, A. Scardicchio, and L. S. Schulman, Zeno dynamics yields ordinary constraints, *Phys. Rev. A* **65**, 012108 (2001).
  - [16] D. Wallace, Simple computer model for the quantum Zeno effect, *Phys. Rev. A* **63**, 022109 (2001).
  - [17] J. B. Mackrory, K. Jacobs, and D. A. Steck, Reflection of a particle from a quantum measurement, *New J. Phys.* **12**, 113023 (2010).
  - [18] G. Gordon, I. E. Mazets, and G. Kurizki, Quantum particle localization by frequent coherent monitoring, *Phys. Rev. A* **87**, 052141 (2013).
  - [19] M. A. Porrás, A. Luis, I. Gonzalo, and A. S. Sanz, Zeno dynamics in wave-packet diffraction spreading, *Phys. Rev. A* **84**, 052109 (2011).

- [20] M. A. Porras, A. Luis, and I. Gonzalo, Quantum Zeno effect for a free-moving particle, *Phys. Rev. A* **90**, 062131 (2014).
- [21] M. A. Porras, N. Mata, and I. Gonzalo, Enhanced quantum tunneling in quantum Zeno dynamics freezing the momentum direction, *Phys. Rev. A* **106**, 012220 (2022).
- [22] See Supplemental Material at <http://link.aps.org/supplemental/10.1103/PhysRevA.109.032207> for the teleportation dynamics.
- [23] G. P. Agrawal, *Nonlinear Fiber Optics* (Academic, New York, 2001).
- [24] M. Majeed and A. Z. Chaudhri, The quantum Zeno and anti-Zeno effects with non-selective projective measurements, *Sci. Rep.* **8**, 14887 (2018).